Radiology

# Cerebellar Cortical Layers: In Vivo Visualization with Structural High-Field-Strength MR Imaging[1]

José P. Marques, PhD
Wietske van der Zwaag, PhD
Cristina Granziera, MD, PhD
Gunnar Krueger, PhD
Rolf Gruetter, PhD

**Purpose:** To perform in vivo imaging of the cerebellum with an in-plane resolution of 120 mm to observe its cortical granular and molecular layers by taking advantage of the high signal-to-noise ratio and the increased magnetic susceptibility-related contrast available at high magnetic field strength such as 7 T.

**Materials and Methods:** The study was approved by the institutional review board, and all patients provided written consent. Three healthy persons (two men, one woman; mean age, 30 years; age range, 28–31 years) underwent MR imaging with a 7-T system. Gradient-echo images (repetition time msec/echo time msec, 1000/25) of the human cerebellum were acquired with a nominal in-plane resolution of approximately 120 μm and a section thickness of 1 mm.

**Results:** Structures with dimensions as small as 240 μm, such as the granular and molecular layers in the cerebellar cortex, were detected in vivo. The detection of these structures was confirmed by comparing the contrast obtained on T2*-weighted and phase images with that obtained on images of rat cerebellum acquired at 14 T with 30 μm in-plane resolution.

**Conclusion:** In vivo cerebellar imaging at near-microscopic resolution is feasible at 7 T. Such detailed observation of an anatomic area that can be affected by a number of neurologic and psychiatric diseases, such as stroke, tumors, autism, and schizophrenia, could potentially provide newer markers for diagnosis and follow-up in patients with such pathologic conditions.



[1] From the Laboratory for Functional and Metabolic Imaging, École Polytechnique Fédérale de Lausanne, Bâtiment CH, Station 6, CH-1015 Lausanne, Switzerland (J.P.M., W.v.d.Z., R.G.); Department of Radiology, University of Lausanne, Lausanne, Switzerland (J.P.M., W.v.d.Z., R.G.); Department of Neurology, Centre Hospitalier Universitaire Vaudois, Lausanne, Switzerland (C.G.); Advanced Clinical Imaging Technology, Siemens Medical Solutions-Centre d'Imagerie BioMédicale, Lausanne, Switzerland (G.K.); and Department of Radiology, University of Geneva, Geneva, Switzerland (R.G.). Received June 25, 2009; revision requested July 28; revision received August 20; accepted September 18; final version accepted October 1. Supported by the Centre d'Imagerie BioMédicale, Université de Lausanne; Université de Genève; Hôpitaux Universitaires de Genève; Centre Hospitalier Universitaire Vaudois; Ecole Polytechnique Fédérale de Lausanne; and the Leenaards and Louis-Jeantet Foundations. **Address correspondence to** J.P.M. (e-mail: *jose.marques@epfl.ch*).

The cerebellum plays a major role not only in movement control but also in cognitive-emotional processing (1,2). Multiple cerebellar functions are integrated in the cortical layer. The convoluted structure of this layer is organized in the folium and is divided into three layers, from the inside to the outside, as follows: granular, Purkinje, and molecular. The cerebellar cortex can be affected by many neurologic and psychiatric diseases, such as stroke, tumors, autism, and schizophrenia (3,4). Also affecting this region are genetic disorders such as ataxias (1) and aceruloplasminemia (5,6), in which layer-dependent variations in iron deposition have been shown using histologic examination (7). Therefore, noninvasive methods delivering precise anatomic images of the cerebellar cortical architecture could potentially provide newer markers for diagnosis and follow-up.

To date, anatomic magnetic resonance (MR) imaging studies of the human cerebellum in vivo have helped supply atlases of the gross anatomic features of the cerebellum (lobules, folia, and fissures) (8) and have been used to describe its complex connectivity (9). Most MR imaging studies are characterized by a spatial resolution on the order of 1 mm and are typically based on T1 contrast, such as that offered by magnetization-prepared rapid acquisition gradient-echo imaging (10). Given the complex and convoluted structure of the cerebellum, such a spatial resolution is inadequate to distinguish the gray matter–white matter boundaries in the cerebellar folia, as well as the different layers that constitute the cerebellar cortex. To our knowledge, such cortical layers have never been observed in vivo with imaging examinations, despite having been observed in vitro as early as in the late 19th century (11).

It has been shown that, when imaging at high field strengths, such as 7 T, T2*-weighted and phase images show superior contrast to that observed on T1-weighted images. This improved contrast is seen not only between white matter and gray matter but also among cortical gray matter layers (12). High-field-strength imaging also allows observation of large heterogeneities within white matter (12,13). This finding is not surprising because the contrast observed in conventional T2*-weighted and phase imaging has a susceptibility origin, and T2*-weighted and phase imaging are therefore expected to increase with increasing magnetic field strength. Furthermore, investigators in a recent study in rats (14) observed cerebellar cortical layers on both phase and T2*-weighted images.

Our hypothesis was that, at 7 T, susceptibility-related contrast in both magnitude and phase gradient-recalled-echo imaging could be used to distinguish the subtle white matter layers interdigitating in the cerebellar folia and the microstructural features of the cerebral human cortex. In addition to the increased contrast and signal available at high field strengths, the higher signal-to-noise ratio achievable with surface coils allows acquisition of images with higher spatial resolution than those achievable at lower field strengths or with volume coils. Achieving such high spatial resolution minimizes partial volume effects that could impair the observation of the individual layers.

The purpose of this study was to take advantage of the high signal-to-noise ratio and the increased magnetic susceptibility-related contrast available at high magnetic field strengths, such as 7 T, to perform in vivo imaging of the cerebellum with an in-plane resolution of 120 mm to observe its cortical granular and molecular layers.

### Advances in Knowledge

- By taking advantage of magnetic susceptibility-related contrast at high field strengths, it is possible to visualize in vivo details of the cerebellar folium and its granular and molecular layers.
- The use of dedicated surface coils allows the acquisition of high-resolution images, on the order of 120-μm in-plane resolution, without problematic artifacts.
- By using the information encoded in the phase images, it is possible to make inferences about increased paramagnetism of structures such as the dentate nucleus and the granular layer of the human cerebellum relative to their surrounding tissues.

## Materials and Methods

One author (G.K.) is an employee of Siemens Medical Solutions, Lausanne, Switzerland, but all other authors had control of the data. The study was approved by the institutional review board of the Faculty of Biology and Medicine at the University of Lausanne, Lausanne, Switzerland, and all subjects provided written consent.

Three healthy subjects (two men, one woman; mean age, 30 years; age range, 28–31 years) underwent imaging with a 7-T 680-mm-bore unit (Magnetom 7T; Siemens Medical Solutions, Erlangen, Germany) equipped with a head gradient insert. A home-built quadrature surface radiofrequency coil (15) that provided excellent coverage of the cerebellum and occipital cortex was used for radiofrequency transmission and reception.

High-resolution gradient-echo images of the human cerebellum were acquired with a nominal in-plane resolution of approximately 120 μm, a section thickness of 1 mm, and a field of view of 115 × 115 mm. A seven-lobe sinc-pulse was used to generate a near-rectangular profile by an MR physicist (W.v.d.Z., with 6 years of imaging experience). Sections were obliquely positioned between coronal and sagittal directions

**Published online**
10.1148/radiol.09091136

**Radiology 2010;** 254:942–948

**Author contributions:**
Guarantors of integrity of entire study, J.P.M., R.G.; study concepts/study design or data acquisition or data analysis/interpretation, all authors; manuscript drafting or manuscript revision for important intellectual content, all authors; approval of final version of submitted manuscript, all authors; literature research, J.P.M., C.G.; experimental studies, J.P.M., W.v.d.Z., C.G., G.K.; and manuscript editing, all authors

See Materials and Methods for pertinent disclosures.

See also the article by Prudent et al and the editorial by Bryan in this issue.

to minimize through-section changes in anatomy by another MR physicist (J.P.M., with 8 years of neuroimaging experience) and a neurologist (C.G., with 7 years of neuroimaging experience), as shown in Fig 1. The acquisition parameters for the gradient-echo acquisition were 1000/25 and an acquisition time of 30 msec per readout. Two repetitions were acquired for each subject, resulting in a total acquisition time of approximately 20 minutes. The nominal flip angle was set to 65° in the region of interest (local flip angle was calculated by using a stimulated-echo acquisition mode [STEAM]–based $B_1$-mapping technique) (16). The echo time was chosen to be approximately equal to the cerebellar T2* for gray matter (approximately 25 msec) to optimize phase (12) and T2* contrast between different cortical layers of gray matter.

A two-dimensional Gaussian high-pass filter with a kernel size of 131 voxels and a width of 10 voxels was applied to the complex images to remove low-frequency phase variations (17) from the resulting phase images (performed by J.P.M). A freely available image processing tool (18) was used to display the images.

The following aspects of images were evaluated: the presence of dipole-like shapes on the phase images and the presence of small structures within the gray matter and white matter of the brain cortex, both in magnitude and phase images (J.P.M.). Regions where section-to-section variations in the anatomic features of the cerebellar cortex were less than 1 pixel over three successive sections were selected for further evaluation (J.P.M. and W.v.d.Z.). The validation of the observation of layers in the cerebellar cortex in both human brain T2*-weighted images and phase images was performed (J.P.M., W.v.d.Z., C.G.) by comparing contrast on those images with the contrast obtained at 14 T in images of a rat brain. Acquisition and evaluation of rat brain images are described in detail elsewhere (14).

## Results

The high-resolution section planes (represented by the white boxes in Fig 1a–1c) were carefully positioned perpendicular to the outer layers of the cerebellar cortex, which were visible on axial lower-resolution images (Fig 1). Because of the complex cerebellar geometry, it was not possible to orient sections so that they were perpendicular to the cerebellar cortex throughout the image.

As can be judged from Fig 2, the cerebellar cortex is approximately three to five times thinner than the cerebral cortex. This finding demonstrates the importance of using very high resolution to depict information about the cortical layer in the cerebellum. The magnitude and phase-contrast images from sections that cross the dentate nucleus, which is well known to have a high iron concentration (11), are shown in Figure 2. As a consequence of its high iron concentration, the dentate nucleus has a low intensity on T2*-weighted images. In the phase images, a magnetic dipolelike effect extending beyond the

**Figure 1**

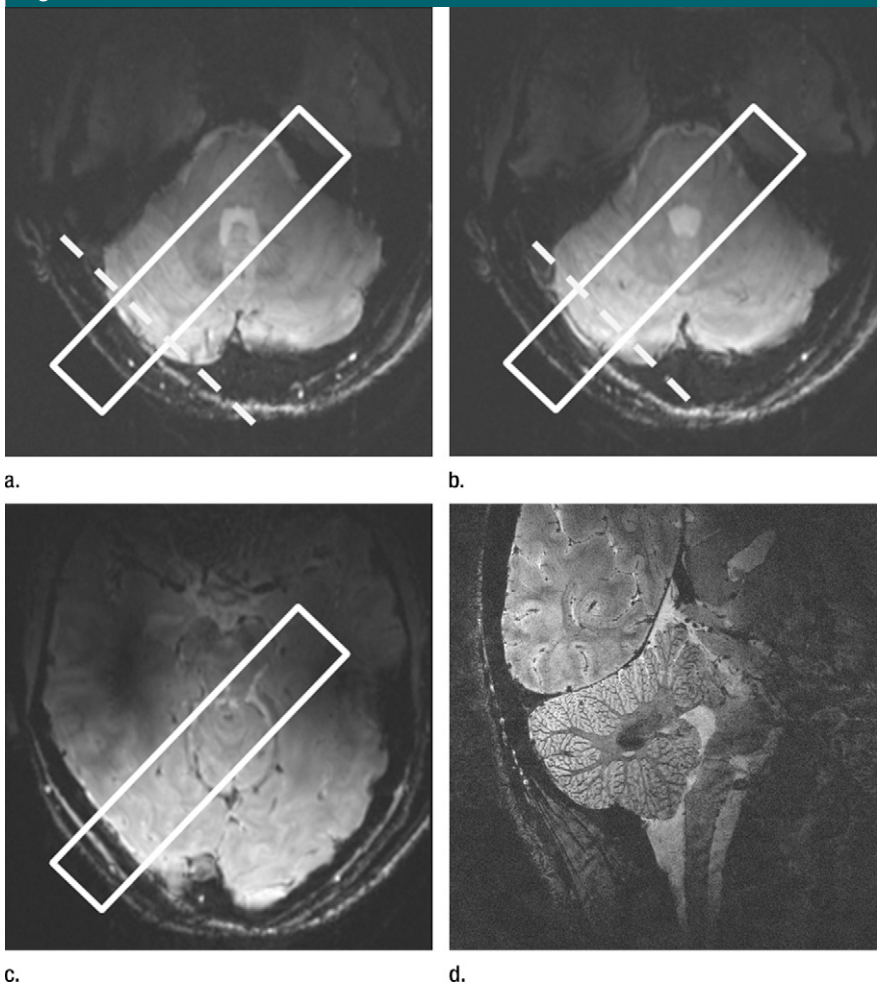


**Figure 1:** **(a–c)** MR images in 28-year-old male volunteer. Transverse low-spatial-resolution multisection gradient-echo images (repetition time msec/echo time msec, 200/5) acquired with 0.6-mm in-plane resolution and 1-mm section thickness were used as anatomic references and to plan the acquisition of subsequent higher-resolution images. Dashed white lines on **a** and **b** indicate estimated main cortical direction and are used to position image volume, represented by white rectangles. **(d)** Representative full-field-of-view high-resolution magnitude gradient-echo image shows from where the anatomic details shown in the subsequent images were highlighted.

nucleus boundary was visible. A positive frequency shift above and below (along the $B_0$ direction) the nucleus and a negative frequency shift surrounding the nucleus in the plane perpendicular to the main static magnetic field was consistently detected. This observation is in agreement with the high iron concentration attributed to the dentate nucleus. Such a dipolelike pattern in the phase images was also apparent in the interfaces between white matter and gray matter, in regions superior to the gray matter folds (white arrows on Fig 2b), with an opposite polarity from that observed surrounding the dentate nucleus. This finding supports the observation that a susceptibility difference between white matter and gray matter is partly responsible for the phase differences (12,14). Some gray matter structures in the brain cortex (black arrows on Fig 2a, 2b) and white-matter structures (black asterisks on Fig 2a, 2b) can be readily observed on both the magnitude and the phase-contrast images. Because of the particular section orientation, which is unlike section orientations used in most clinical studies (12,19) (ie, not perpendicular to the magnetic field), small veins passing through the white matter toward the cortex exhibited a negative frequency shift (14) and thus appear bright on the phase-contrast image (white asterisk on Fig 2b).

Given the complex anatomic structure of the cerebellum, maintaining an orthogonal orientation of the section orientation in respect to cerebellar structures was possible only in parts of the sections. Nonetheless, in the 18 sections in the high-resolution data, it was possible to determine regions where the boundaries between white matter and gray matter remained constant in the through-section direction and thus where the cerebellar cortex was perpendicular to the section direction. Magnitude and phase images of those regions of interest (Fig 3b–3e) show white matter bundles conveying into the cerebellar folium that appear dark on the magnitude images and bright on the phase image. Conversely, when compared with the white matter, the two layers of the cerebellar cortex appear brighter on the magnitude images and darker on the phase images. Two layers, granular and molecular, within the cerebellar cortex were distinguishable, mainly because of the phase contrast; compared with the molecular layer, the granular layer had a strong positive frequency shift. Both the magnitude and the phase contrast between those two layers in humans was in good agreement with that observed in the rat brain (Fig 4) (14). By using the scale bars, we estimated that the granular layer had a dimension of approximately 240–300 μm and that of the molecular layer varied from 240 to 500 μm, values in good agreement with the histologic literature (20).

**Figure 2**

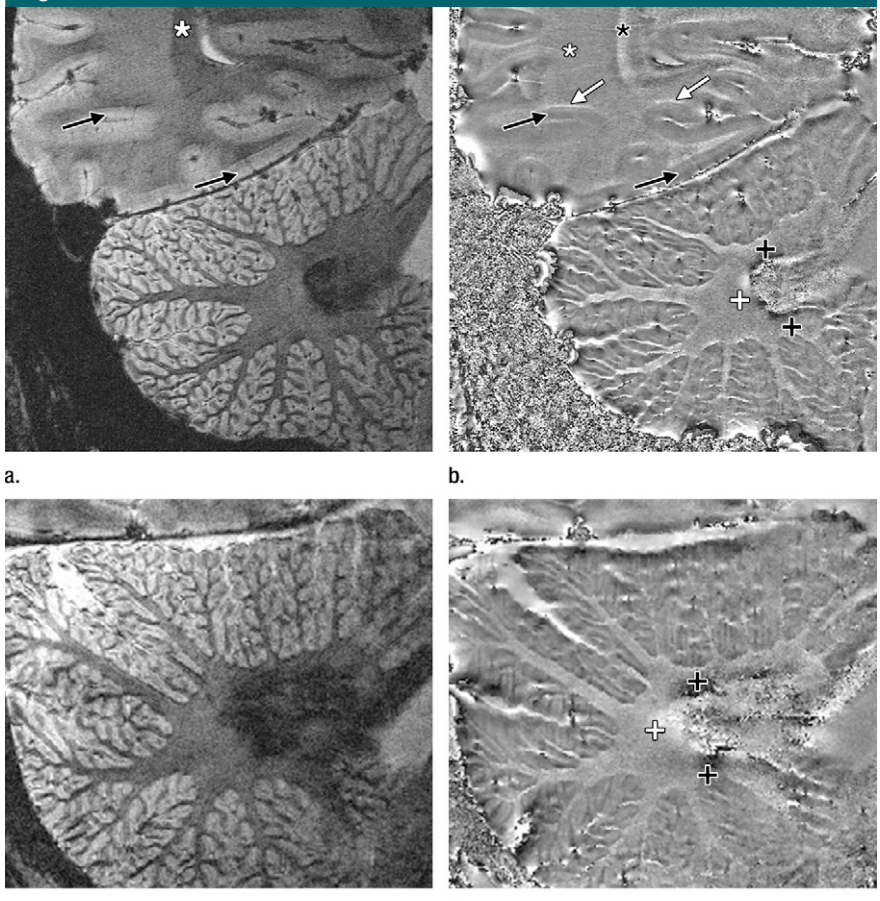


**Figure 2:** High-resolution **(a, c)** magnitude and **(b, d)** phase gradient-echo data from two volunteers (31-year-old male and 30-year-old female volunteers, respectively) show sections crossing dentate nucleus. Phase images show expected dipole shape surrounding the dentate nucleus, which is a structure known to have a high iron concentration. Calipers = positive and negative lobes of the dipole shape, respectively. White arrows = negative frequency shifts in regions superior to interfaces of gray matter and white matter. Black arrows = observable cortical gray matter structure. * = regions where white matter bundles are observable both in magnitude and phase images.

## Discussion

Very high magnetic field strength (>3 T) combined with a dedicated local radiofrequency coil allowed acquisition of human in vivo images of the cerebellum (120-μm in-plane spatial resolution) that depicted cortical layers (about 240 μm thick) in the cerebellar folium.

**Figure 3**

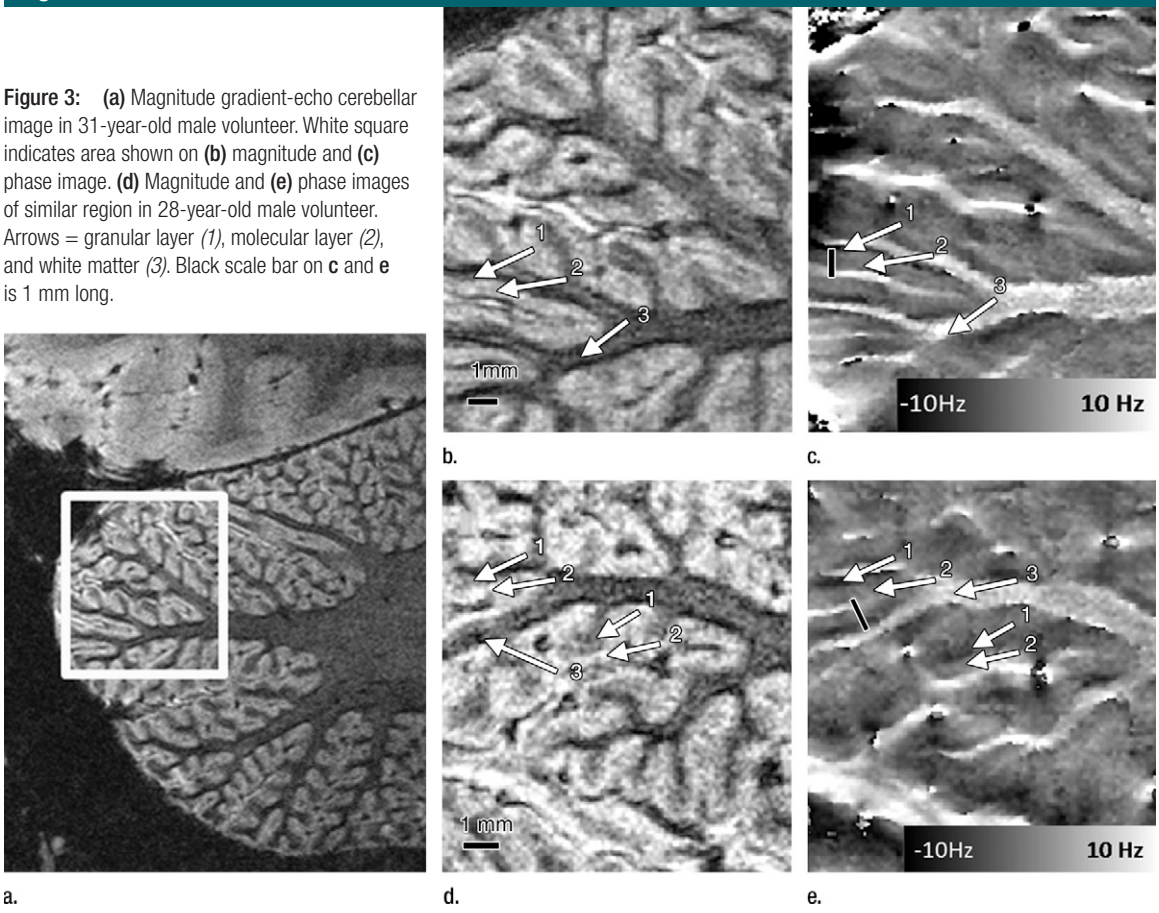


**Figure 3:** **(a)** Magnitude gradient-echo cerebellar image in 31-year-old male volunteer. White square indicates area shown on **(b)** magnitude and **(c)** phase image. **(d)** Magnitude and **(e)** phase images of similar region in 28-year-old male volunteer. Arrows = granular layer *(1)*, molecular layer *(2)*, and white matter *(3)*. Black scale bar on **c** and **e** is 1 mm long.

**Figure 4**

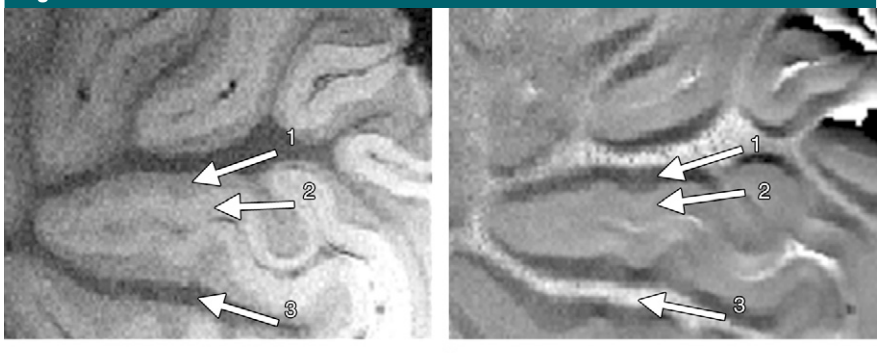


**Figure 4:** **(a)** In vivo magnitude and **(b)** phase gradient-echo images of rat cerebellum acquired at 14 T. The main image and acquisition variables are as follows: 1100/16; in-plane resolution, 30 μm; and section thickness, 0.4 mm. Acquisitions were averaged over approximately 60 minutes (14). Arrows = granular layer *(1)*, molecular layer *(2)*, and white matter *(3)*. To allow better comparison with images in Figure 3, these images were reoriented so that the main magnetic field is pointing in the vertical direction (as in the human data). (Adapted and reprinted, with permission, from reference 14.)

The high-resolution images were devoid of notable imaging artifacts, such as motion artifacts. This finding was ascribed in part to the sensitivity of the surface radiofrequency coil—it was low in distal regions of increased flow or movement (such as the left and right internal carotid arteries, the jaw, the throat, and the nose cavity). Further reduction in artifacts might be associated with using the surface coil to also perform transmission; this not only allowed the use of a reduced field of view but also decreased the magnetization that was excited in distal parts of the brain, which could have propagated artifacts into the field of view. Although the same resolution may be obtained in whole-brain data through parallel imaging, the use of a transmit-receive surface coil eliminates the need for parallel imaging and thus the risk of associated artifacts (21).

Despite the long acquisition time used in the current protocol (30 msec, which is on the order of magnitude of cortical gray matter T2* at 7 T [22]), the effective resolution in the readout direction will be affected by only 4% (23). Although respiration-related artifacts

were not clear in our data, frequency variations of up to 7 Hz are expected at the cerebellar region at 7 T (24). Such fluctuations in frequency could be overcome by real-time shimming (25) or section dynamic shimming (26).

The high-resolution images show two cortical layers in vivo, which were tentatively assigned to the granular and the molecular layers, respectively. The same structures were more clearly visible in the rat cerebellum because of the longer acquisition time, higher resolution, and even higher $B_0$ of 14 T available for the rat images. Higher resolution would be needed to depict the Purkinje cell layer, which is expected to be approximately 12 μm wide (27). We showed that the phase contrast of the cerebellar layers, particularly the granular layer, depended on orientation. This finding suggests that the phase difference of the granular layer and neighboring tissues is largely caused by susceptibility variations. The high amplitude in the phase-contrast images suggests that this layer is highly paramagnetic compared with most brain tissues, which might be related to the high iron concentration observed in the granular layer with use of Perl staining (7). The same can be said of the dentate nucleus, which is a known feature from previous studies (28). To evaluate the extent of their paramagnetism, it would be necessary to compute susceptibility maps (29–31). Such maps would give information that could correlate with iron concentration (14). Future studies could exploit this potential as a diagnostic marker of cerebellar diseases that affect the iron regulation of the cerebellum (7) and to monitor therapeutic interventions.

Isotropic resolution would be preferable in applications in which a quantitative susceptibility distribution is to be calculated or if the aim were to observe the cerebellar cortical layers throughout the whole cerebellum. With our current setup, the same signal-to-noise ratio could theoretically be obtained with an isotropic resolution of 0.24 mm. Although the signal-to-noise ratio would remain unchanged, the in-plane resolution might be insufficient to allow a clear visualization of the cortical layers. The need to obtain three-dimensional images would imply a greater sensitivity to physiological noise. In the future, performing a more thorough and comprehensive study of the substructures of the cerebellum will require redefining the imaging variables to enable coverage of the entire cerebellum.

We conclude that high-field-strength systems allow in vivo detection of the microanatomic features of complex structures such as the cerebellar folia because of the high resolution and contrast attainable on T2*-weighted and phase-contrast images. The anatomic features of the cerebellum can be affected by a number of neurologic and psychiatric diseases, such as stroke, tumors, autism, and schizophrenia (3,4). The capability to noninvasively image this region of the brain could potentially provide newer markers for diagnosis and follow-up in patients with these conditions.

**Acknowledgments:** The authors thank Martin Hergt, MSc, Advanced Clinical Imaging Technology, Siemens Medical Solutions-Centre d'Imagerie BioMédicale, Lausanne, Switzerland, and Arthur Magill, PhD, Department of Radiology, University of Lausanne, Lausanne, Switzerland, for building and optimizing the surface coil.

## References

1. Schmahmann JD. Disorders of the cerebellum: ataxia, dysmetria of thought, and the cerebellar cognitive affective syndrome. J Neuropsychiatry Clin Neurosci 2004;16:367–378.
2. Schmahmann JD, Caplan D. Cognition, emotion and the cerebellum. Brain 2006; 129:290–292.
3. Schmahmann JD, Weilburg JB, Sherman JC. The neuropsychiatry of the cerebellum—insights from the clinic. Cerebellum 2007;6: 254–267.
4. Steinlin M. Cerebellar disorders in childhood: cognitive problems. Cerebellum 2008; 7:607–610.
5. Grisoli M, Piperno A, Chiapparini L, Mariani R, Savoiardo M. MR imaging of cerebral cortical involvement in aceruloplasminemia. AJNR Am J Neuroradiol 2005;26:657–661.
6. Stankiewicz J, Panter SS, Neema M, Arora A, Batt CE, Bakshi R. Iron in chronic brain disorders: imaging and neurotherapeutic implications. Neurotherapeutics 2007;4:371–386.
7. Patel BN, Dunn RJ, Jeong SY, Zhu Q, Julien JP, David S. Ceruloplasmin regulates iron levels in the CNS and prevents free radical injury. J Neurosci 2002;22:6578–6586.
8. Schmahmann JD, Doyon J, McDonald D, et al. Three-dimensional MRI atlas of the human cerebellum in proportional stereotaxic space. Neuroimage 1999;10:233–260.
9. Granziera C, Schmahmann JD, Hadjikhani N, et al. Diffusion spectrum imaging shows the structural basis of functional cerebellar circuits in the human cerebellum in vivo. PLoS One 2009;4:e5101.
10. Mugler JP 3rd, Brookeman JR. Three-dimensional magnetization-prepared rapid gradient-echo imaging (3D MP RAGE). Magn Reson Med 1990;15:152–157.
11. Voogd J. The human cerebellum. J Chem Neuroanat 2003;26:243–252.
12. Duyn JH, Van Gelderen P, Li TQ, De Zwart JA, Koretsky AP, Fukunaga M. High-field MRI of brain cortical substructure based on signal phase. Proc Natl Acad Sci U S A 2007;104:11796–11801.
13. Rauscher A, Sedlacik J, Barth M, Mentzel HJ, Reichenbach JR. Magnetic susceptibility-weighted MR phase imaging of the human brain. AJNR Am J Neuroradiol 2005;26:736–742.
14. Marques JP, Maddage R, Mlynarik V, Gruetter R. On the origin of the MR image phase contrast: an in vivo MR microscopy study of the rat brain at 14.1 T. Neuroimage 2009;46:345–352.
15. Adriany G, Gruetter R. A half-volume coil for efficient proton decoupling in humans at 4 tesla. J Magn Reson 1997;125:178–184.
16. Stollberger R. aBT. In-vivo assessment of a STEAM sequence for B1-mapping [abstr]. In: Proceedings of the Sixteenth Meeting of the International Society for Magnetic Resonance in Medicine. Berkeley, Calif: International Society for Magnetic Resonance in Medicine, 2008; 3091.
17. Noll DC, Nishimura DG, Macovski A. Homodyne detection in magnetic resonance imaging. IEEE Trans Med Imaging 1991; 10:154–163.
18. Smith SM, Jenkinson M, Woolrich MW, et al. Advances in functional and structural MR image analysis and implementation as FSL. Neuroimage 2004;23 (suppl 1): S208–S219.
19. Haacke EM, Xu Y, Cheng YC, Reichenbach JR. Susceptibility weighted imaging (SWI). Magn Reson Med 2004;52:612–618.

20. Andersen BB, Gundersen HJ, Pakkenberg B. Aging of the human cerebellum: a stereological study. J Comp Neurol 2003;466:356–365.

21. Pruessmann KP, Weiger M, Scheidegger MB, Boesiger P. SENSE: Sensitivity encoding for fast MRI. Magn Reson Med 1999;42:952–962.

22. Peters AM, Brookes MJ, Hoogenraad FG, et al. T2* measurements in human brain at 1.5, 3 and 7 T. Magn Reson Imaging 2007;25:748–753.

23. Haacke M, Brown R, Thompson M, et al. Magnetic resonance imaging: physical principles and sequence design. New York, NY: Wiley-Liss, 1999.

24. Van de Moortele PF, Pfeuffer J, Glover GH, Ugurbil K, Hu X. Respiration-induced B0 fluctuations and their spatial distribution in the human brain at 7 Tesla. Magn Reson Med 2002;47:888–895.

25. Van Gelderen P, De Zwart JA, Starewicz P, Hinks RS, Duyn JH. Real-time shimming to compensate for respiration-induced B0 fluctuations. Magn Reson Med 2007;57:362–368.

26. Koch KM, McIntyre S, Nixon TW, Rothman DL, de Graaf RA. Dynamic shim updating on the human brain. J Magn Reson 2006;180:286–296.

27. Strassle BW, Menegola M, Rhodes KJ, Trimmer JS. Light and electron microscopic analysis of KChIP and Kv4 localization in rat cerebellar granule cells. J Comp Neurol 2005;484:144–155.

28. Sehgal V, Delproposto Z, Haacke EM, et al. Clinical applications of neuroimaging with susceptibility-weighted imaging. J Magn Reson Imaging 2005;22:439–450.

29. Cheng YC, Neelavalli J, Haacke EM. Limitations of calculating field distributions and magnetic susceptibilities in MRI using a Fourier based method. Phys Med Biol 2009;54:1169–1189.

30. Marques JP, Bowtell R. Application of a fourier-based method for rapid calculation of field inhomogeneity due to spatial variation of magnetic susceptibility. Concepts Magn Reson Part B Magn Reson Eng 2005;25B:65–78.

31. Liu T, Spincemaille P, de Rochefort L, Kressler B, Wang Y. Calculation of susceptibility through multiple orientation sampling (COSMOS): a method for conditioning the inverse problem from measured magnetic field map to susceptibility source image in MRI. Magn Reson Med 2009;61:196–204.